Label-free DNA biosensor based on a peptide nucleic acid-functionalized microstructured optical fiber-Bragg grating

Alessandro Candiani
Alessandro Bertucci
Sara Giannetti
Maria Konstantaki
Alex Manicardi
Stavros Pissadakis
Annamaria Cucinotta
Roberto Corradini
Stefano Selleri

Label-free DNA biosensor based on a peptide nucleic acid-functionalized microstructured optical fiber-Bragg grating

Alessandro Candiani,[a] Alessandro Bertucci,[b] Sara Giannetti,[a] Maria Konstantaki,[c] Alex Manicardi,[b] Stavros Pissadakis,[c] Annamaria Cucinotta,[a] Roberto Corradini,[b] and Stefano Selleri[a]
[a]University of Parma, Department of Information Engineering, Area Parco delle Scienze 181/A, 43124, Parma, Italy
[b]University of Parma, Department of Chemistry, Area Parco delle Scienze 17/A, 43124 Parma, Italy
[c]Foundation for Research and Technology—Hellas FORTH, Institute of Electronic Structure and Laser IESL, Vassilika Vouton, 700 13 Heraklion, Crete, Greece

Abstract. We describe a novel sensing approach based on a functionalized microstructured optical fiber-Bragg grating for specific DNA target sequences detection. The inner surface of a microstructured fiber, where a Bragg grating was previously inscribed, has been functionalized by covalent linking of a peptide nucleic acid probe targeting a DNA sequence bearing a single point mutation implicated in cystic fibrosis (CF) disease. A solution of an oligonucleotide (ON) corresponding to a tract of the CF gene containing the mutated DNA has been infiltrated inside the fiber capillaries and allowed to hybridize to the fiber surface according to the Watson-Crick pairing. In order to achieve signal amplification, ON-functionalized gold nanoparticles were then infiltrated and used in a sandwich-like assay. Experimental measurements show a clear shift of the reflected high order mode of a Bragg grating for a 100 nM DNA solution, and fluorescence measurements have confirmed the successful hybridization. Several experiments have been carried out on the same fiber using the identical concentration, showing the same modulation trend, suggesting the possibility of the reuse of the sensor. Measurements have also been made using a 100 nM mismatched DNA solution, containing a single nucleotide mutation and corresponding to the wild-type gene, and the results demonstrate the high selectivity of the sensor. © 2013 Society of Photo-Optical Instrumentation Engineers (SPIE) [DOI: 10.1117/1.JBO.18.5.057004]

Keywords: biosensors; DNA detection; cystic fibrosis; microstructured optical fibers; optical fiber sensor; Bragg gratings; peptide nucleic acid; gold nanoparticles.

Paper 12827R received Dec. 28, 2012; revised manuscript received Apr. 5, 2013; accepted for publication Apr. 12, 2013; published online May 10, 2013.

1 Introduction

The need for new, fast, and cheap technologies for medical and healthcare diagnostic equipment has been driving interest and investment in biosensor technology and research.[1] Among the different principles of detection, optical-based biosensing is one of the most widely investigated transduction methods. In particular, optical fiber sensors offer the main advantage of small and flexible shape, connecting a remote light source to a small in situ sensing element; they are able to give rapid and sensitive detection of the target in real time, especially if the detection is performed using a label-free scheme. Microstructured optical fibers (MOFs), also called photonic crystal fibers (PCFs), are characterized by a pattern of air holes running along the entire length of the fiber. Since their discovery,[2] they have represented a versatile photonic platform for many sensing applications, by infiltrating the specimen to be tested inside their capillaries. This approach is particularly advantageous in biosensing, since small biological samples inside the holes can be probed by the guided light inside the holes. Theoretical studies have been carried out demonstrating the feasibility and the high potential of this technology for sensing applications.[3,4]

Various research groups have implemented a very attractive and interesting class of MOF-based sensors for bio-applications. Jensen et al.[5] described a sensor for detection of biomolecules in an aqueous solution using a PCF without a solid core. By infiltrating fluorophore-labeled DNA in the air holes of the microstructured part of a PCF, the transmission peak located in the absorption region of the fluorophore revealed the presence of the target biomolecule. Ruan et al.[6] used soft glass MOFs to detect quantum dot-labeled proteins, achieving a detection limit of 1 nM. Afshar et al.[7] developed a generic model of excitation and fluorescence recapturing, supported by the experimental results, within filled solid-core MOFs. The strong overlap with the evanescent wave penetrating into the holes hosting the sample under test is one of the main characteristic of the PCF-based sensing technology. The more the core diameter of the fiber decreases, the more the overlap grows. In addition, the small core can actually be an advantage for approaches exploiting the inherent nonlinearity of the PCF, like the four-wave mixing-based biosensor first proposed in Ref. 8 and recently experimentally demonstrated in Ref. 9. Polymeric MOFs, which have attractive material and biochemical properties, have been also used successfully in such a photonic

approach for biosensing. The first demonstration of biosensing with a polymer MOF was in 2005, in which the Polymethylmethacrylate microstructured fiber was used for fluorescence-based selective detection of the antibody streptavidin.[10] Emiliyanov et al.[11,12] presented a microstructured polymer optical fiber (mPOF) fabricated from Topas cyclic olefin copolymer, where localized sensor layers could be activated on the inner side of the air holes in a predetermined section of the fiber, and the detection of fluorophore-labeled antibodies was proven. Moving on label-free techniques, different approaches can be implemented to detect specific biological targets; Markos et al.[13] realized a dual-core mPOF biosensor that detects change of the layer thickness of antibody biomolecules by monitoring the change in the coupling length between the two cores. Furthermore, long period gratings (LPGs) in microstructured fibers have been utilized by Rindorf et al.[14] where by observing the shift of the resonant peak of a LPG it was possible to measure the thickness of a monolayer of poly-L-lysine and double-stranded DNA. One of the major challenges in DNA detection is the discrimination of different sequences differing only for a single nucleobase, i.e., point mutations or single nucleotide polymorphisms. This characteristic is particularly important since point mutations can be related to genetic diseases, such as cystic fibrosis (CF) or thalassemia, and are frequently found in the DNA of tumor cells.[15]

In this work we report for the first time to our knowledge, a new DNA sensing approach based on a peptide nucleic acid (PNA)-functionalized MOF Bragg grating. By employing Bragg gratings instead of LPGs the signal is monitored in reflection mode allowing the use of the fiber as probe. Theoretical models have been developed to characterize Bragg gratings as transduction elements in PCFs biosensors.[16,17] Here we demonstrate experimentally the feasibility of such a scheme adopting the following approach. The inner surface of "grapefruit" geometry MOF has been functionalized using PNA probe, an oligonucleotide (ON) mimic that is well suited for specific DNA target sequences detection. In our case the DNA sequence of the CF gene containing a point mutation was chosen as test model. After the solution of DNA molecules had been infiltrated inside the fiber capillaries and hybridization had occurred, oligonucleotide-functionalized gold nanoparticles (ON-AuNPs) were added and used to form a sandwich-like system to achieve signal amplification, as observed in other optical techniques.[18] Spectral measurements of the reflected signal show a clear wavelength shift of the high order mode band for a 100 nM DNA solution. Several experiments have been carried out on the same fiber demonstrating the reproducibility of the results and the selectivity of the sensor.

2 Experimental Section

2.1 Microstructured Optical Fiber-Bragg Grating

The MOF used in this experiment was 25.8 cm long with grapefruit geometry, having five holes of 20.8 μm diameter, forming an outer core of 16.1 μm, which includes a 3.5%wt Ge doped socket of diameter 8.5 μm, as shown in Fig. 1(a). In that fiber, a 22-mm-long Bragg grating was inscribed using a 1067.73 nm phase mask and a 193 nm excimer laser, 10 ns laser radiation.[19] The grating reflected two major modes, located at 1546 nm (0th order) and 1541.6 nm (1st order), with strengths 25 and 12 dB, respectively. Profile beam measurements showed that the 0th order mode is confined into the Ge-doped core, while the 1st order mode is defined by the surrounding capillary structure, extending to a greater area, as shown in the Fig. 1(b) and 1(c). The inscription of the grating caused a slight birefringence effect in the fiber, and this was observed in the high order mode spectrum, Fig. 1(d), that showed double peak.

2.2 Materials and Reagents

All reagents were obtained from commercial suppliers and used without further purification. Hydrocloric acid 37%, sodium hydrogen carbonate, and sodium chloride were purchased from VWR (Italy). Methanol, ethanol, acetonitrile, sodium dodecylsulfate, succinic anhydride, N,N-dimethylformamide (DMF), N,N-diisopropylcarbodiimide (DIC), N,N-diisopropylethylamine (DIPEA), N-hydroxysuccinimide (NHS), (3-aminopropyl)triethoxysilane (APTES), tris(hydroxymethyl)aminomethane (Tris),
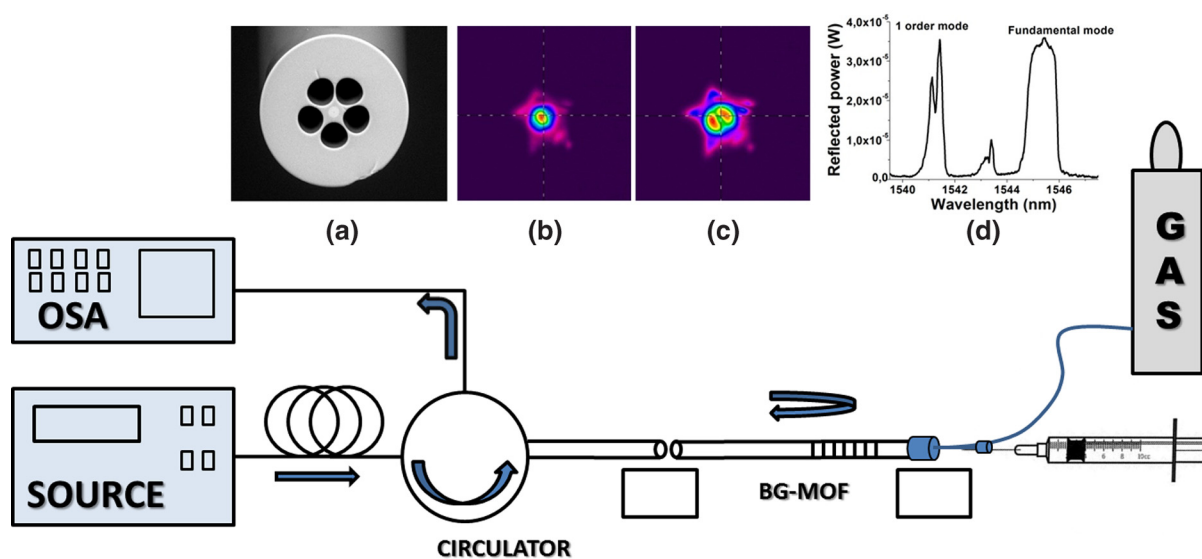

Fig. 1 The schematic of the optical setup implemented for the experiment is presented. In the top graph, (a) a scanning electron microscope photo of the microstructured optical fiber (MOF) used, with (b) the fundamental and (c) the first order beam profiles. (d) The reflected spectrum of the MOF, revealing a slight birefringence effect.

trifluoroacetic acid (TFA), tetrachloroauric(III) acid, and ethylenediaminetetraacetic acid were purchased from Sigma-Aldrich (Italy). Ethanolamine, trisodium citrate, and Rink amide resin were purchased from Merck (Italy). Sodium hydroxide in pellets was purchased from Carlo erba (Italy). Fmoc-C(Bhoc)-OH, Fmoc-G(Bhoc)-OH, Fmoc-T-OH, Fmoc-AEEA-OH were all purchased from ASM (Germany). Fmoc-A(Bhoc)-OH was purchased from Link Technologies (UK). HBTU was purchased from Matrix Innovation (Canada). Wild-type streptavidin was purchased from Invitrogen (Italy). Biotinylated and fluorescently labeled ONs were purchased from Thermo Fisher Scientific. Ultra-pure water (Milli-Q Element, Millipore) was used for all the experiments.

2.3 Microstructured Optical Fiber Functionalization

As described in a previous work,[3] the most stable modification for an optical fiber silica surface can be obtained by tethering of biomolecules or other probes through a silanization procedure. Briefly, the protocol used is described by the following steps:

1. Cleaning and activation of the silica surface with treatment with HCl:Methanol 1:1 for 30 min.

2. Silanization with APTES 5% in ethanol, overnight.

3. Reaction of the amino group with succinic anhydride 0.25 M in DMF in order to obtain a carboxylic acid functional group attached to the surface, overnight.

4. Activation of the carboxylic function with DIC and NHS in DMF as solvent, 0.25 M both, overnight.

5. Reaction of the activated ester with the end terminal amino group of the PNA probe, 30 μM in 100 mM carbonate buffer in H_2O:ACN = 9:1, 0.001% sodium dodecylsulfate, pH = 9, overnight. Silica-DNA binding is shown in Fig. 2(a).

6. Quenching of the excessive activated esters with ethanolamine 50 mM in aqueous Tris buffer pH = 9, for 3 h.

Internal derivatization was obtained by applying a nitrogen pressure of 2 atm to an in-house built apparatus comprised by a PTFE tubing reservoir containing the solutions, connected to the end of the fiber through a HPLC PEEK ferrule junction. After each treatment, the fiber was washed with the corresponding solvent, and the liquid was completely removed by a nitrogen flux.

The actual success of the derivatization procedure was then tested by hybridization experiments with a labeled full-complementary ON to the PNA probe sequence. Measurements were carried out by using a ScanArray Express (Perkin Elmer, Waltham, Massachusetts), which performed fluorescence scanning of the fibers deposited on glass slides.

2.4 PNA Oligomer Synthesis

The synthesis of the PNA was performed on a Syro I fully automated peptide synthesizer (Biotage, Uppsala, Sweden) in a 5 μmol scale by using Fmoc chemistry using two equivalent/ double coupling protocol, with HBTU/DIPEA coupling and a Rink amide resin, loaded with Fmoc-PNA-T-OH as first

monomer. The crude PNA oligomer was then purified by RP-HPLC with UV detection at 260 nm (510 HPLC Pumps and 2487 Dual λ Absorbance Detector, Waters, Milford, Massachusetts) with use of a semipreparative XTerra Prep RP18 column (7.8 × 300 mm, 10 μm, Waters), with a gradient elution from 100% A (0.1% TFA in water) to 100% B (0.1% TFA in acetonitrile) in 30 min; flow rate was 4 ml/min. The resulting pure PNA was characterized by HPLC-DAD-ESI-MS (Alliance 2695, 996 Photodiode Array, Waters and Quattro micro API, Micromass), by using a Phenomenex Jupiler C18 column (5 μm, 4.6 × 250 nm, 300 Å), with a gradient elution from 100% A (0.2% FA in water) to 50% B (0.2% FA in acetonitrile) in 30 min. ESI-MS: m/z found (calcd): 533.7 (533.8) $[M + 8H]^{8+}$, 609.9 (610.0) $[M + 7H]^{7+}$, 711.4 (711.5) $[M + 6H]^{6+}$, 853.7 (853.6) $[M + 5H]^{5+}$.

The purified PNA was quantified by UV-Vis spectroscopy (Lambda BIO 20, Perkin-Elmer) by UV absorbance using the following $\varepsilon_{260}(M^{-1} cm^{-1})$ for the nucleobases: T 8600, C 6600, A 13700, G 11700, which gave a concentration of 971.6 μM for a 1 mL sample, corresponding to 971.6 nmol (19% yield).

2.5 Preparation of Oligonucleotide-Functionalized Gold Nanoparticles

Gold nanoparticles (AuNPs) were synthesized by citrate reduction of HAuCl$_4$ according to the methods elsewhere described.[20] The AuNPs were then characterized by UV-vis spectroscopy[21] and a mean diameter of 13 ± 3 nm was found. In order to obtain the final conjugation with a 16-mer biotinylated ON, AuNPs were firstly coated with streptavidin using the following procedure: 1 ml of a diluted colloidal solution of AuNPs (absorbance 0.2) was incubated for 1 h at 4°C with 20 μL of a 1 mg/ml streptavidin aqueous solution, then pH was adjusted to 8.5 with NaOH and an overnight incubation at 4°C was carried out. Thus, a purple pellet was obtained by centrifugation (3390 rcf, 30 min) and finally resuspended in 500 μL H$_2$O. Conjugation with the biotinylated DNA sequence was carried out by adding 20 μL of a 100 μM aqueous solution of the biotinylated ON to the streptavidin coated AuNPs; after 30 min of incubation at room temperature, the solution was centrifuged (845 rcf, 30 min) and the resulting pellet was resuspended in 100 μL phosphate buffer solution (PBS), pH = 7.

2.6 Optical Set-Up

An amplified stimulated emission (ASE) source (ASE 1600, NTT Electronics), used as a broadband light source, was connected to a fiber optic circulator 1 × 2 (1530 to 1570 nm bandwidth), as shown in Fig. 1. The light was coupled to the functionalized MOF through the port2 of the circulator, and the reflected signal was analyzed though the port3 using an optical spectrum analyzer (Ando AQ-6315A). The functionalization of the microcapillaries and DNA infiltration process were performed by infiltrating the reagents in the holes of the MOF using a syringe pump (KD Scientific 100 series). The system was connected to a high pressure micro-filtered nitrogen line, to empty and dry the fiber after infiltration. In order to make the setup even more reliable, a high precision dynamometer was also used to keep the fiber always with the same tension. The measurements were made in a clean room environment with a temperature control system. Spectral measurements of the reflected signal have been recorded at the beginning and at the end of
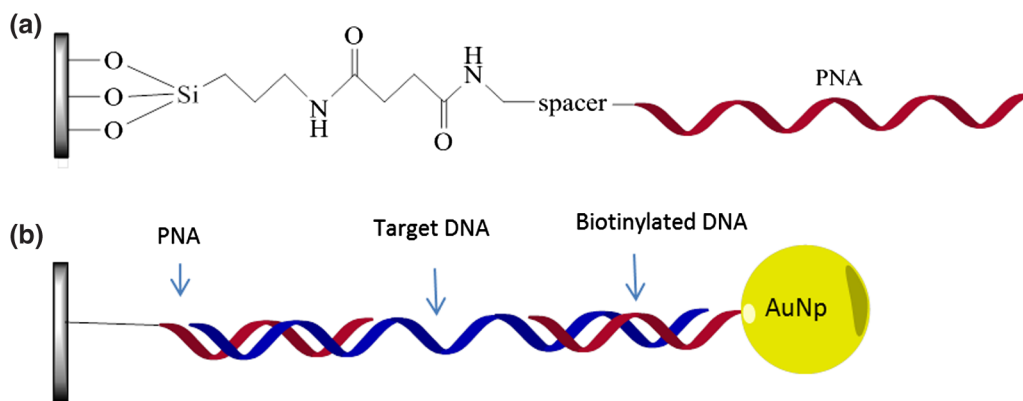
Fig. 2 (a) Scheme of the final linkage of the peptide nucleic acid (PNA) probe to the fiber internal surface and (b) scheme of the sandwich-like system used for DNA detection.

every hybridization phase. In Fig. 1, the whole experimental setup is represented.

3 Results and Discussion

To test the functionalization process and the binding of PNA probes to the internal surface of the fiber channels, hybridization experiments were carried out using a fluorescently labeled full complementary ON (DNA-FM-Cy3), whose sequence is reported in Table 1. The sequences used were chosen in order to mimic the DNA sequence bearing a single point mutation (W1282X) which is implicated in CF disease,[22] which is the most common mutation present on 50% to 60% of CF chromosomes in the Ashkenazi Jewish population, and was previously studied by our group.[23] The PNA probe used is targeted to the mutated sequence, and ideally should give low or no response to the wild type DNA, thus revealing only the presence of the mutated sequence.

To assess the ability of the modified surface to capture complementary DNA, the PNA-modified microstructured fiber and a nonfunctionalized one were filled with a solution of fluorescently labeled DNA-FM-Cy3. The two fibers were both infiltrated for 50 min by using the syringe pump with an aqueous solution 100 nM of the Cy3-labeled ON, whose

sequence is perfectly full matched with the PNA probes attached on the silica surface. Then, the fibers were dried with a nitrogen flux, washed with excess PBS and dried again. The two fibers were fixed on a glass slide and a fluorescent image was achieved by means of the microarray fluorescence reader, using a laser source of 543 nm for the excitation of the Cy3 fluorophore. By evaluating the fluorescence intensity from the ScanArray image through the instrument software, the signal-to-noise ratio of the modified fiber, with respect of the background of the plane glass slide, was found to be almost 140; the signal arising from the PNA-modified fiber was found almost nine folds more intense than that obtained for the nonderivatized one, as reported in Fig. 3, thus demonstrating the actual success of the functionalization procedure and, at the same time, the great ability of the PNA probes to bind to the complementary DNA strand. The higher fluorescent signal in the derivatized fiber is due to the capture of DNA by PNA probes on the inner fiber surfaces, whereas the residual fluorescence in the unmodified fiber is caused only by nonspecific adsorption on the silica surface. Although in some protocols bovine serum albumin (BSA) is used as blocking agent in order to reduce nonspecific interactions,[24] we evaluated that gold-nanoparticle BSA interactions[25] could produce unspecific binding during the final detection step; therefore, only passivation of active sites with ethanolamine was used.

In the label-free detection experiment, unmodified DNA bearing the point mutation and a sequence for AuNP capture was used. Before the infiltration of the DNA solutions, PBS was infiltrated into the microcapillaries to evaluate the stability of the signal, which remained unchanged for the duration of approximately 1 h. The syringe pump was used for infiltrating the DNA inside the fiber at a fixed flow rate of 0.25 μL/ min, ensuring a

Table 1 Sequences of the PNA probe and DNA target. In bold the base corresponding to the W1282X point mutation, in italics the target sequence for oligonucleotide-functionalized gold nanoparticle (ON-AuNP) are indicated.

Oligo	Sequence	Role
PNA	H-O-O-CTTTCCT**T**CACTGTT-NH$_2$	Probe
DNA-FM-Cy3	Cy3-GCAACAGTG**A**AGGAAAGCC	Cy3 full-match
DNA-FM	*ATCGATGGTGTGTCTT*GGGATTCA ATAACTTTGCAACAGTG**A**AGGAAAG	Unlabeled full-match (CF mutation)
DNA-MM	*ATCGATGGTGTGTCTT*GGGATT CAATAACTTTGCAACAGTG**G**A GGAAAG	Unlabeled single base mismatch (wild type)
AuNP-DNA	AAGACACACCAT CGAT— BIOTIN	Biotinylated DNA for AuNP functionalization

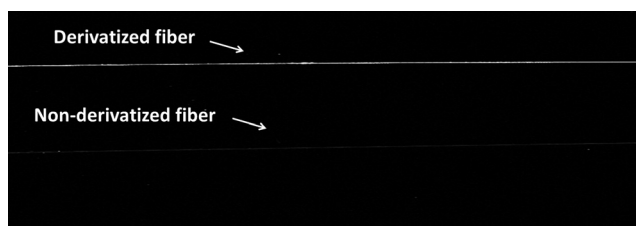Note: O: 2-(2-aminoethoxy)ethoxyacetyl spacer.

Fig. 3 ScanArray Express image of an unmodified fiber (below) and a PNA-derivatized fiber (above) after infiltration of the fluorescently labeled full complementary oligonucleotide (ON) (DNA-FM-Cy3).
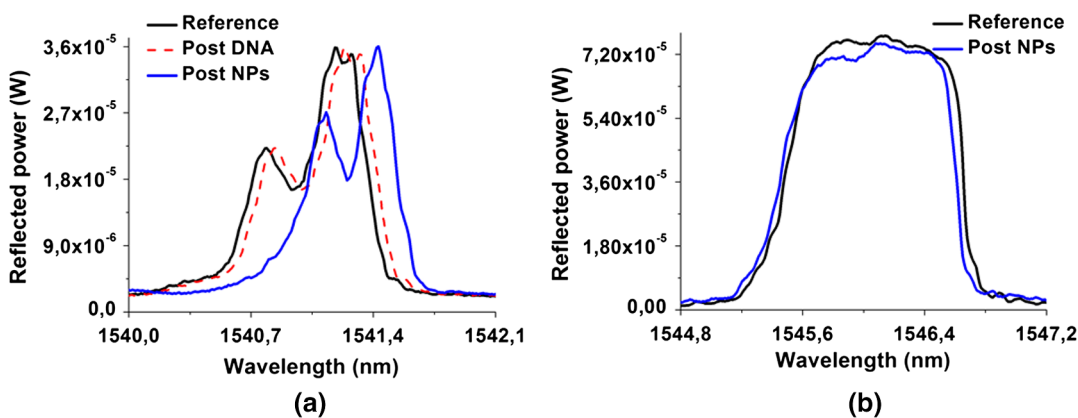
Fig. 4 Spectral measurements after the hybridization process with 100 nM full-match DNA solution and gold nanoparticles NPs. (a) A clear red shift was recorded for the higher order mode, (b) while the fundamental mode did not record any significant change.
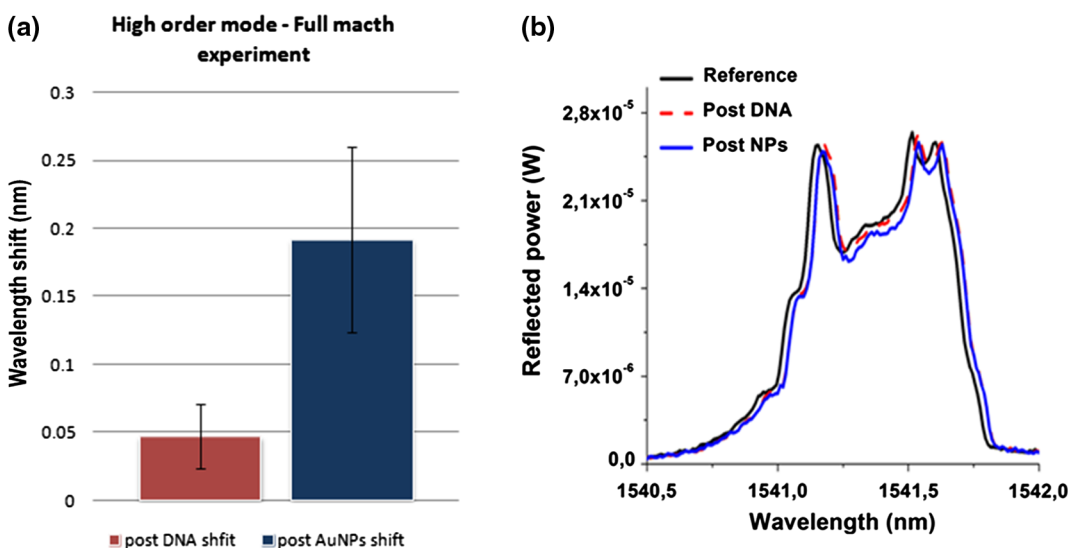

Fig. 5 (a) Average of the high order wavelength shift after DNA infiltration (red) and after oligonucleotide-functionalized gold nanoparticles (ON-AuNPs) infiltration (blue); a small memory effect decreases the modulation observed for each experiment performed on the same fiber. (b) Spectral measurements after the hybridization process using 100 nM mismatch DNA solution and gold NPs.

continuous renewal of the DNA solution in contact with the surface. The 100 nM DNA solution was infiltrated through the fiber capillaries for 1 h, and then the fiber was emptied using nitrogen at 5 atm. The reflected signal after the infiltration of DNA-FM showed a small shift of 0.05 nm in the higher order, as illustrated in the red dash line in Fig. 4. When the DNA binds to the PNA, it replaces buffer solution molecules within a few nanometers from the surface of the fiber, resulting in a refractive-index change near the sensor surface. At this low DNA concentration, the captured DNA layer is not thick enough to be optically detected as shift in the reflected signal, in accordance with results obtained for other optical biosensors based on fiber gratings and a similar functionalization.[26,27] Subsequently, to enhance the measured shift, the ON-AuNPs solution was infiltrated for 1 h, and then the fiber was washed with PBS and emptied again. The last process allows the golden NPs to bind to the DNA target, increasing the refractive index contrast between the silica surface of the capillaries and the analyte [see Fig. 2(b)]. The maximum shift observed for the reflected high order band in this experiment was around 0.27 nm towards the red, whereas no

significant changes were observed in the fundamental mode, as reported in Fig. 4. The binding of the gold nanoparticles to their target on the DNA captured on the fiber greatly amplify the response of the fiber, since the layer deposited onto the fiber channel surface is greatly incremented, thereby increasing the effective refractive index of the fiber, n_{eff}. This effect is translated into a shift of the reflected high order Bragg peak, as described by the Bragg condition. In this case, the shift was statistically significant, as reported in Fig. 4(a). This discrepancy between the two modes was supported by initial experiments on the spectral sensitivity of the two Bragg grating modes where liquids of different refractive indices were infiltrated in the capillaries. Measurements revealed that the high order mode is one order of magnitude more sensitive to refractive index changes with respect to the fundamental mode (results not shown) supporting the theoretical calculations of beam profiles illustrated in Fig. 1(b) and 1(c).

Several measurements were carried out using the same functionalized fiber in order to evaluate the repeatability of the device. We used the 100 nM DNA solution to verify the

reproducibility of a single measurement. The recovery of the fiber was achieved by washing the fiber capillaries with PBS for approximately 24 h with a pressure of 10 atm. The removal of DNA was confirmed spectrally since the reflected signal had shifted back to its initial reference position. Three more rehybridization processes were implemented using the same conditions described earlier, showing very similar results, except for a small memory effect, similar to that previously observed,[26] which tends to decrease the amplitude modulation with the number of tests carried out. The average wavelength shift of the high order mode was 0.04 ± 0.02 nm after DNA hybridization, and 0.19 ± 0.06 nm ($n = 3$, RSD% = 35%) after NPs hybridization, as reported in Fig. 5.

Finally, the sequence-selectivity of the fiber was tested using the mismatched ON (DNA-MM), corresponding to wild type DNA differing of only one base from DNA-FM, but bearing exactly the same target sequence for ON-AuNP. Using the same procedure described above, a 100 nM mismatch DNA solution was infiltrated into the functionalized capillaries, the capillary was washed and then infiltrated with ON-AuNP, after which a spectral measurement was performed. The experiments showed that the total shift was 0.025 nm, as shown in Fig. 5(b), much lower than that obtained using FM-DNA. After the measurement, the same fiber was washed with PBS, dried, and the hybridization experiment was repeated using DNA-FM; the response was a final shift of 0.11 nm, absolutely consistent with the former ones, thus confirming the sequence-selectivity of the optical response.

4 Conclusion

In this work, a novel DNA biosensing approach based on Bragg grating inscribed in a PCF has been presented for the first time, to the best of our knowledge. The fiber was previously functionalized and showed discrimination at the single-base level. The optical device showed a small shift of the reflected high order Bragg mode when DNA molecules, complementary to the PNA probes, were infiltrated into the MOF; however, by "decoration" of the captured DNA with gold nanoparticle, a significant shift was observed only in the case of full match DNA. This first demonstration proves the feasibility of realizing a sensor for biological measurements observing the signal reflected by a Bragg grating, utilizing the fiber itself as a probe. The fiber used in the experiment shows a good compromise between size of the holes, sensitivity and relative ease of inscription of the grating. The approach can be extended to more other fibers with improved sensitivity to local refractive index changes, thus increasing the signal modulation. Other recognition elements able to bind target analytes, such as proteins or contaminants, can be introduced using the same strategy as described here, thus making this technology suitable for powerful and versatile biosensing platforms.

References

1. J. H. T. Loung, K. B. Male, and J. Glennon, "Biosensor technology: technology push versus market pull," *Biotechnol. Adv.* **26**(5), 492–500 (2008).
2. J. C. Knight et al., "All-silica single-mode optical fiber with photonic crystal cladding," *Opt. Lett.* **21**(19), 1547–1549 (1996).
3. E. Coscelli et al., "Toward a highly specific DNA biosensor: PNA-modified suspended-core photonic crystal fibers," *IEEE J. Sel. Top. Quant. Electron.* **16**(4), 967–972 (2010).
4. D. Passaro et al., "All-silica hollow-core microstructured Bragg fibers for biosensor application," *IEEE Sens. J.* **8**(7), 1280–1286 (2008).
5. J. B. Jensen et al., "Photonic crystal fiber based evanescent-wave sensor for detection of biomolecules in aqueous solutions," *Opt. Lett.* **29**(17), 1974–1976 (2004).
6. Y. Ruan et al., "Detection of quantum-dot labelled proteins using soft glass microstructured optical fibers," *Opt. Express* **15**(26), 17819–17826 (2007).
7. V. S. Afshar, S. C. Warren-Smith, and T. M. Monro, "Enhancement of fluorescence-based sensing using microstructured optical fibers," *Opt. Express* **15**(26), 17891–17901 (2007).
8. J. R. Ott et al., "Label-free and selective nonlinear fiber-optical biosensing," *Opt. Express* **16**(25), 20834–20847 (2008).
9. M. H. Frosz, A. Stefani, and O. Bang, "Highly sensitive and simple refractive index sensing of liquids in photonic crystal fibers using four-wave mixing," *Opt. Express* **19**(11), 10471–10484 (2011).
10. J. B. Jensen et al., "Selective detection of antibodies in microstructured polymer optical fibers," *Opt. Express* **13**(15), 5883–5889 (2005).
11. G. Emiliyanov et al., "Localized biosensing with Topas microstructured polymer optical fiber," *Opt. Lett.* **32**(5), 460–462 (2007).
12. G. Emiliyanov et al., "Localized biosensing with Topas microstructured polymer optical fiber: erratum," *Opt. Lett.* **32**(9), 1059–1059 (2007).
13. C. Markos et al., "Label-free biosensing with high sensitivity in dual-core microstructured polymer optical fibers," *Opt. Express* **19**(8), 7790–7798 (2011).
14. L. Rindorf et al., "Photonic crystal fiber long-period gratings for biochemical sensing," *Opt. Express* **14**(18), 8224–8231 (2006).
15. C. Greenman et al., "Patterns of somatic mutation in human cancer genomes," *Nature* **446**(7132), 153–158 (2007).
16. N. Burani and J. Lægsgaard, "Perturbative modeling of Bragg-grating-based biosensors in photonic-crystal fibers," *J. Opt. Soc. Am. B* **22**(11), 2487–2493 (2005).
17. L. Rindorf and O. Bang, "Sensitivity of photonic crystal fiber grating sensors: biosensing, refractive index, strain, and temperature sensing," *J. Opt. Soc. Am. B* **25**(3), 310–324 (2008).
18. R. D'Agata et al., "Ultrasensitive detection of DNA by PNA and nanoparticle-enhanced surface plasmon resonance imaging," *Chem. Biochem.* **9**(13), 2067–2070 (2008).
19. S. Pissadakis, M. Livitziis, and G. D. Tsibidis, "Investigations on the Bragg grating recording in all-silica, standard and microstructured optical fibers using 248 nm 5 ps, laser radiation," *J. Eur. Opt. Soc. Rap. Public.* **4**, 09049 (2009).
20. K. C. Grabar et al., "Preparation and characterization of Au colloid monolayers," *Anal. Chem.* **67**(4), 735–743 (1995).
21. W. Haiss et al., "Determination of size and concentration of gold nanoparticles from UV–vis spectra," *Anal. Chem.* **79**(11), 4215–4221 (2007).
22. T. Shoshani et al., "Association of a nonsense mutation (W1282X), the most common mutation in the Ashkenazi Jewish cystic fibrosis patients in Israel, with presentation of severe disease," *Am. J. Hum. Genet.* **50**(1), 222–228 (1992).
23. R. Corradini et al., "Enhanced recognition of cystic fibrosis W1282X DNA point mutation by chiral peptide nucleic acids probes by a surface plasmon resonance biosensor," *J. Mol. Rec.* **17**(1), 76–84 (2004).
24. X. T. Zheng and C. M. Li, "Single living cell detection of telomerase over-expression for cancer detection by an optical fiber nanobiosensor," *Biosens. Bioelectron.* **25**(6), 1548–1552 (2010).
25. K. Vangala et al., "Studying protein and gold nanoparticle interaction using organothiols as molecular probes," *J. Phys. Chem. C* **116**(5), 3645–3652 (2012).
26. A. Candiani et al., "Optical fiber ring cavity sensor for label-free DNA detection," *IEEE J. Sel. Top. Quant. Electron.* **18**(3), 1176–1183 (2012).
27. M. Sozzi et al., "Modification of a long-period grating based fiber optic for DNA biosensing," *Proc. SPIE* **7894**, 7894–7820 (2011).